Diagnostic Accuracy Study

Medicine®

OPEN

Differences and prediction of imaging characteristics of COVID-19 and non-COVID-19 viral pneumonia

A multicenter study

Bo Zhang, MD[a], Xia Wang, MD[a], Xiaoyan Tian, MD[a], Xiaoying Zhao, PhD[a], Bin Liu, PhD[a], Xingwang Wu, PhD[a,*], Yaqing Du, MD[b], Guoquan Huang, MD[c], Qing Zhang, MD[d]

Abstract

To study the differences in imaging characteristics and prediction of COVID-19 and non-COVID-19 viral pneumonia through chest CT.

Chest CT data of 128 cases of COVID-19 and 47 cases of non-COVID-19 viral pneumonia confirmed by several hospitals were retrospectively collected, the imaging performance was evaluated and recorded, different imaging features were statistically analyzed, and a prediction model and independent predicted imaging features were obtained by multivariable analysis.

COVID-19 was more likely than non-COVID-19 pneumonia to have a high-grade ground glass opacities ($P = .01$), extensive lesion distribution ($P < .001$), mixed lesions of varying sizes (27.7% vs 57.0%, $P = .001$), subpleural prominence (23.4% vs 86.7%, $P < .001$), and lower lobe prominence (48.9% vs 82.0%, $P < .001$). However, peribronchial interstitial thickening was more likely to occur in non-COVID-19 viral pneumonia (36.2% vs 19.5%, $P = .022$). The statistically significant differences from multivariable analysis were the degree of ground glass opacities ($P = .001$), lesion distribution ($P = .045$), lesion size ($P = .020$), subpleural prominence ($P < .001$), and lower lobe prominence ($P = .041$). The sensitivity and specificity of the model were 94.5% and 76.6%, respectively, with an AUC of 0.91.

The imaging characteristics of COVID-19 and non-COVID-19 viral pneumonia are different, and the prediction model can further improve the specificity of chest CT diagnosis.

Abbreviations: AUC = area under the ROC curve, COVID-19 = Coronavirus Disease 19, CT = computed tomographic, GGO = ground-glass opacities, MERS = middle east respiratory syndrome, ROC = receiver operating characteristic, RT-PCR = reverse transcription polymerase chain reaction, SARS = severe acute respiratory syndrome, WHO = World Health Organization.

Keywords: computed tomography, COVID-19, pneumonia, specificity

1. Introduction

By the end of December 2019, novel coronavirus 2019 pneumonia (COVID-19) began in Wuhan, Hubei, China, and spread rapidly on a large scale worldwide. By the beginning of March 2020, COVID-19 had reached 114 countries, affected more than 100,000 people and killed more than 4000 people. On March 12, 2020, the World Health Organization defined COVID-19 as a pandemic.[1] Although the virus causing COVID-19, SARS-COV-2, belongs to the same genus as SARS-COV and MERS-COV, its transmissibility and case fatality rate are quite different. The binding capacity of the surface S protein on SARS-COV-2 to angiotensinase 2 is approximately 10 to 20 times that of SARS-COV,[2] so its infectivity is significantly higher than that of SARS-COV. The case fatality rate of COVID-19 (3%–4%) is lower than that of SARS (10%) and MERS (approximately 36%), but it is significantly higher than that of H1N1 virus (0.1%–1%).[3–5] The early symptoms of the disease are mainly fever and cough, and some patients progress to severe acute respiratory distress syndrome and respiratory failure, as well as different degrees of involvement of systemic organs.[6,7]

Early detection, early isolation and timely treatment are the key points for the prevention and treatment of the epidemic. RT-PCR and chest CT in the early period are the main means for the early detection of the disease. The sensitivity of RT-PCR was reported to be lower than that of chest CT.[8] Due to the sampling method, supply shortage and other reasons, it is difficult for the first RT-PCR to achieve timely and accurate diagnosis in a large number of suspected patients, which leads to a large number of missed diagnoses and increases the risk of transmission. COVID-19 overlaps with other non-COVID-19 viral pneumonias in terms of

Editor: Hyunjin Park.

The authors report no conflicts of interest.

The datasets generated during and/or analyzed during the current study are available from the corresponding author on reasonable request.

[a] Department of Radiology, The First Affiliated Hospital of Anhui Medical University, [b] Department of Imaging, Fuyang Second People's Hospital, [c] Department of Imaging, Wuhu Second People's Hospital, [d] Department of imaging, Luian People's Hospital China.

[*] Correspondence: Xingwang Wu, Department of Radiology, The First Affiliated Hospital of Anhui Medical University, China, 218ji-xi road, Hefei 230022, China (e-mail: duobi2004@126.com).

How to cite this article: Zhang B, Wang X, Tian X, Zhao X, Liu B, Wu X, Du Y, Huang G, Zhang Q. Differences and prediction of imaging characteristics of COVID-19 and non-COVID-19 viral pneumonia: a multicenter study. Medicine 2020;99:42(e22747).

Received: 28 April 2020 / Received in final form: 19 August 2020 / Accepted: 11 September 2020

http://dx.doi.org/10.1097/MD.0000000000022747

imaging findings. In addition, when the patients exposure history is unclear, it is difficult for diagnostic imaging doctors to distinguish the 2. Accurate diagnosis requires subjective experience, and failure to make a timely or accurate diagnosis increases the risk of epidemic spread or excessive medical treatment. Nonviral pneumonia is easy to differentiate on imaging, and coupled with laboratory examination, clinician diagnosis is not difficult. In this study, we analyzed the characteristics of COVID-19 and other viral pneumonias on chest CT for the first time and made a COVID-19 prediction model based on these analyses. This method can effectively exclude subjective factors to make predictions and distinctions, and especially when the patient's contact history is unclear, it can quantify the incidence probability of COVID-19 relative to that of other viral pneumonias to improve the specificity of chest CT.

2. Materials and methods

2.1. Study population

The clinical history data of 132 cases of COVID-19 diagnosed in several hospitals from January to February 2020 and 76 cases of non-COVID-19 viral pneumonia diagnosed clinically from January 2016 to December 2019 were retrospectively collected. Four CT-negative COVID-19 cases and 29 cases with other viral pneumonia without a nucleic acid test or viral antibody test were excluded. The final number of cases included was 128 COVID-19 and 47 non-COVID-19 viral pneumonias. The first chest CT images of all patients after symptom onset were collected and recorded. Each hospitals ethics committee approved the study.

2.2. CT examination method

All patients were scanned by 2 scanners: a 64-MDCT Light Speed VCT (GE healthcare) and Somatom Emotion (Siemens healthcare). The collection parameters were set to 120 kVp, 100 to 200 mAs, spacing of 0.75 to 1.5, and collimating of 0.625 to 5 mm. All imaging data were reconstructed using the reconstruction algorithm of medium sharpness, and the thickness of the layers was 0.625 to 5 mm. CT images were obtained in the supine position with complete inspiration.

2.3. Image analysis and evaluation

Two radiologists with 10 years of radiographic experience independently assessed the images without prior knowledge of the clinical diagnosis. Differences between the 2 radiologists were resolved by consensus to achieve consistent results. All images were evaluated at the axial position under the lung window (width, 1600 HU; level, -600 HU) and the mediastinal window (width, 400 HU; level, 40 HU). The following imaging features were recorded:

1. consolidation degree and ground glass opacity degree (grade 0: less than 10% of all lesions; grade 1 accounted for 30% of all lesions; grade 2 accounted for 30%–60% of all lesions; grade 3 accounted for 60%–90% of all lesions; and grade 4 accounted for greater than 90% of all lesions);
2. main lesion morphology (nodular, patchy, or large patchy);
3. lesion distribution (localized or small, scattered, multiple, or diffuse);
4. lesion size (small lesion less than 3 cm, large lesion more than 3 cm, or mixed lesions);
5. air bronchogram;
6. fibrotic streaks;
7. subpleural prominence (lesions located mainly in the subpleural space);
8. distribution along the bronchovascular bundle;
9. interlobular septal or reticular thickening;
10. peribronchovascular interstitial thickening (CT demonstrates vascular thickening or bronchial wall thickening);
11. pleural thickening;
12. lower lobe prominence (lesions located mainly in the lower lobe); 13. total number of involved lung lobes; and
13. distribution of lesions in different lung lobes.

2.4. Statistical analysis

SPSS statistical software (version 25.0; SPSS Inc., Chicago, Illinois, United States) was used for analysis. Continuous variables are expressed as averages ± standard deviations and compared by the Mann–Whitney U test. Categorical variables are expressed as numbers and percentages and are compared by the Chi-Squared test or Fishers exact test. $P < .05$ was considered statistically significant. The results of univariate analysis ($P < .05$) and clinically significant factors ($P > .05$) were included in the multivariable analysis. Multivariable analysis and prediction models were established by binary logistic regression. A receiver operating characteristic (ROC) curve was used to evaluate the performance of the prediction model.

3. Results

3.1. Clinical characteristics

The distribution of non-COVID-19 viral pneumonia pathogens is shown in Figure 1, including 16 cases of influenza A, 9 cases of cytomegalovirus (CMV), 8 cases of Epstein-Barr virus (EBV), 5 cases of adenovirus, 4 cases of influenza B, 3 cases of human parainfluenza virus (HPIV) and 2 cases of varicella-zoster virus (VZV). COVID-19 patients included 79 males and 49 females, with an average age of 46.1 ± 12.8 years. Twenty one males and 26 females were included in the non-COVID-19 viral pneumonia group, with an average age of 41.9 ± 23.1 years. Men were more common in the COVID-19 group than in the non-COVID-19 group (61.7%, $P = .045$). The average time between symptom onset and initial CT examination was 7.0 ± 4.3 days for non-COVID-19 viral pneumonia and 6.0 ± 3.4 days for COVID-19. The main clinical features of the 2 groups are summarized in Table 1. The main symptoms were fever, cough, sore throat, fatigue, and muscle soreness.

3.2. Imaging features

The imaging characteristics of non-COVID-19 viral pneumonia and COVID-19 are shown in Table 2. The main COVID-19 imaging characteristics included grade-3 ground glass opacities (52 [40.6%]), large patchy lesions (71 [55.5%]), multiple lesions (73 [57.0%]), mixed lesions (73 [57.0%]), air bronchograms (30 [23.4%]), fibrotic streaks (47 [36.7%]), subpleural prominence (111 [86.7%]), distribution along the bronchovascular bundle (29 [22.7%]), interlobular septal, or reticular thickening (41 [32.0%]), peribronchovascular interstitial thickening (25 [19.5%]), and pleural thickening (31 [24.2%]); the average number of involved lung lobes was 3.6 ± 1.6; and the lower lobe

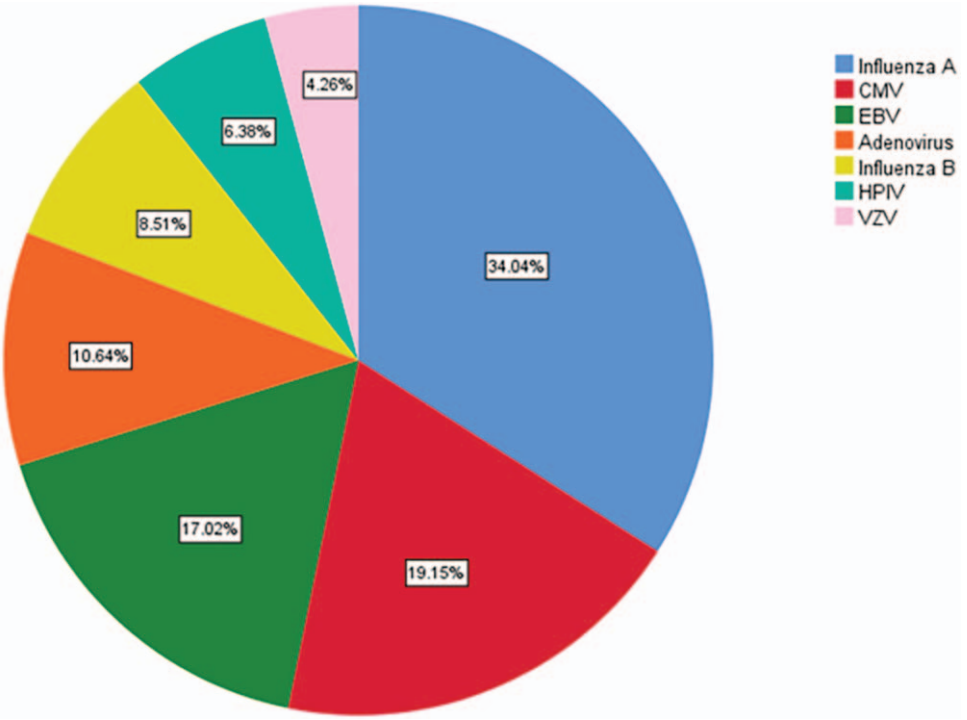

Figure 1. The distribution of non-COVID-19 viral pneumonia pathogens.

was prominent (105 [82%]). Compared with non-COVID-19 viral pneumonia, COVID-19 was more likely to have high-grade ground glass opacities ($P = .010$) (Fig. 2**AD**), a wide distribution of lesions ($P < .001$), mixed lesions of different sizes (27.7% vs 57.0%, $P = .001$) (Fig. 2CE), subpleural prominence (23.4% vs 86.7%, $P < .001$) (Fig. 2ABCE), and lower lobe prominence (48.9% vs 82.0%, $P < .001$) (Fig. 2FG). However, peribronchial interstitial thickening was more likely to occur in non-COVID-19 viral pneumonia (36.2% vs 19.5%, $P = .022$) (Fig. 2CGH). The distribution of lesions in different lung lobes is shown in Figure 3. In both COVID-19 and non-COVID-19 viral pneumonia, the right lower lobe (83.6% and 76.6%) was more involved than the other lobes. The left upper lobe was more involved in COVID-19 than in non-COVID-19 viral pneumonia (74.2% vs 57.4%, $P = .032$). After adjusting for confounding factors by binary logistic regression analysis, independent predicted factors were identified (Table 3), including the degree of ground glass opacities ($P = .001$), lesion distribution ($P = .045$), lesion size ($P = .020$), subpleural prominence ($P < .001$), and lower lobe prominence ($P = .041$). The prediction model established by logistic regression was statistically significant; the Chi-Squared value was 94.016, $P < .001$; the area under the ROC curve (AUC) (Fig. 4) was 0.91; the specificity was 76.6%; the sensitivity was 94.5%; and the accuracy was 89.7%.

4. Discussion

COVID-19, a highly infectious and high-mortality infectious disease, has become a global epidemic. Early diagnosis and recognition of the disease are the keys to controlling the epidemic. Although the diagnosis of COVID-19 depends on RT-PCR, the sensitivity of the first RT-PCR of sputum and throat swab tests is approximately 50%- to 70%, while that of chest CT is over 90%.[8–10] As a noninvasive examination method, chest CT can

Table 1

Clinical characteristics of non-COVID-19 and COVID-19.

Clinical symptoms	no-COVID-19 (n = 47)	COVID-19 (n = 128)	χ^2 / Z	*P*
Fever	35 (74.5)	113 (88.2)	5.027	.025*
Cough	30 (63.8)	96 (75.0)	2.128	.145
Sore throats	13 (27.7)	15 (11.7)	6.500	.110
Fatigue	13 (27.7)	32 (25.0)	0.127	.721
Muscle pain	12 (25.5)	24 (18.8)	0.968	.325
Abdominal pain, diarrhea	5 (10.6)	18 (14.1)	0.353	.552
Vomiting	1 (3.0)	5 (3.9)	0.328	.567
The time from symptom onset to the first CT scan mean (SD)	7.02 (4.31)	6.01 (3.42)	−1.244†	.214

* indicate significant *P* value.
† Z value (Mann–Whitney U test).

Table 2

Comparison of image characteristics of non-COVID-19 virus and COVID-19.

Characteristics	no-COVID-19 (n = 47)	COVID-19 (n = 128)	χ^2 / Z	P
Age mean (SD)	41.9 (23.1)	46.1 (12.8)	−1.211†	.226
Sex			4.003	.045*
Male	21 (44.7)	79 (61.7)		
Female	26 (55.3)	49 (38.3)		
Consolidation degree			7.718	.093
0	6 (12.8)	34 (26.6)		
1	16 (34.0)	52 (40.6)		
2	6 (12.8)	13 (10.2)		
3	15 (31.9)	24 (18.8)		
4	4 (8.5)	5 (3.9)		
GGO degree			12.872	.010*
0	6 (12.8)	5 (3.9)		
1	15 (31.9)	24 (18.8)		
2	6 (12.8)	13 (10.2)		
3	16 (34.0)	52 (40.6)		
4	4 (8.5)	34 (26.6)		
Main lesion morphology			5.256	.069
Nodular	12 (25.5)	20 (15.6)		
Patchy	18 (38.3)	37 (28.9)		
Large patchy	17 (36.2)	71 (55.5)		
Lesion distribution			37.066	<.001*
Localized or small	3 (6.4)	28 (21.9)		
Scattered	22 (46.8)	19 (14.8)		
Multiple	11 (23.4)	73 (57.0)		
Diffuse	11 (33.4)	8 (6.3)		
Lesion size			12.892	.002*
Small lesion	17 (36.2)	33 (25.8)	1.818	.178
Large lesion	17 (36.2)	22 (17.2)	7.153	.007*
Mixed lesion	13 (27.7)	73 (57.0)	11.866	.001*
Air bronchogram	11 (23.4)	30 (23.4)	0.000	.996
Fibrotic streaks	17 (36.2)	47 (36.7)	0.004	.947
Subpleural prominence	11 (23.4)	111 (86.7)	65.27	<.001*
Distribution along the bronchovascular bundle	12 (25.5)	29 (22.7)	0.158	.691
Interlobular septal or reticular thickening	11 (23.4)	41 (32.0)	1.225	.268
Peribronchovascular interstitial thickening	17 (36.2)	25 (19.5)	5.218	.022*
Pleural thickening	15 (31.9)	31 (24.2)	1.051	.305
Total lobe involvement	3.5 (1.6)	3.6 (1.6)	−0.407†	.684
Lower lobe prominent	23 (48.9)	105 (82.0)	19.167	<.001*

* indicate significant *P* value.
† Z value (Mann–Whitney U *test*).
GGO = ground glass opacities.

quickly and conveniently screen suspected cases and act as an important complementary examination method for RT-PCR in epidemic areas. However, the specificity of chest CT is only 25%,[8,10,11] which leads to the emergence of a large number of false positive patients, bringing a certain sense of panic to the patients and placing a certain burden on medical management. When the infection source exposure history is unclear, it is difficult to distinguish COVID-19 from other viral pneumonias, as there are many similarities in imaging manifestations, while bacterial pneumonia is easy to distinguish via laboratory blood cell examination.[12] By analyzing the imaging manifestations of COVID-19 and non-COVID-19 viral pneumonia, this study identified the relatively statistically significant imaging feature differences, calculated the independently predicted imaging features excluding confounding factors through a multivariable binary logistic regression equation, and established a relevant prediction model based on the factors included in the regression equation.

According to this multicenter study of 128 COVID-19 cases, we found that COVID-19 early imaging features include mainly an increased degree of ground glass opacities, main large patchy lesions, mixed lesions and multiple lesions, air bronchogram, fibrotic streaks, subpleural prominence, distribution along the bronchovascular bundle, interlobular septal or reticular thickening, peribronchovascular interstitial thickening, pleural thickening, and lower lobe prominence. These findings are broadly similar to those previously reported in the literature. However, interlobular septal thickening and bronchial interstitial thickening occurred less in our study than in previous reports,[4–14] which may be related to the fact that our case collection represents the first chest CT examination of the patients, and the pathological changes are still in the early stage, such as the imaging features of lobular septal thickening and bronchial and vascular thickening not appearing. Our study also found that compared with non-COVID-19 viral pneumonia patients, COVID-19 patients were more likely to have high-grade ground

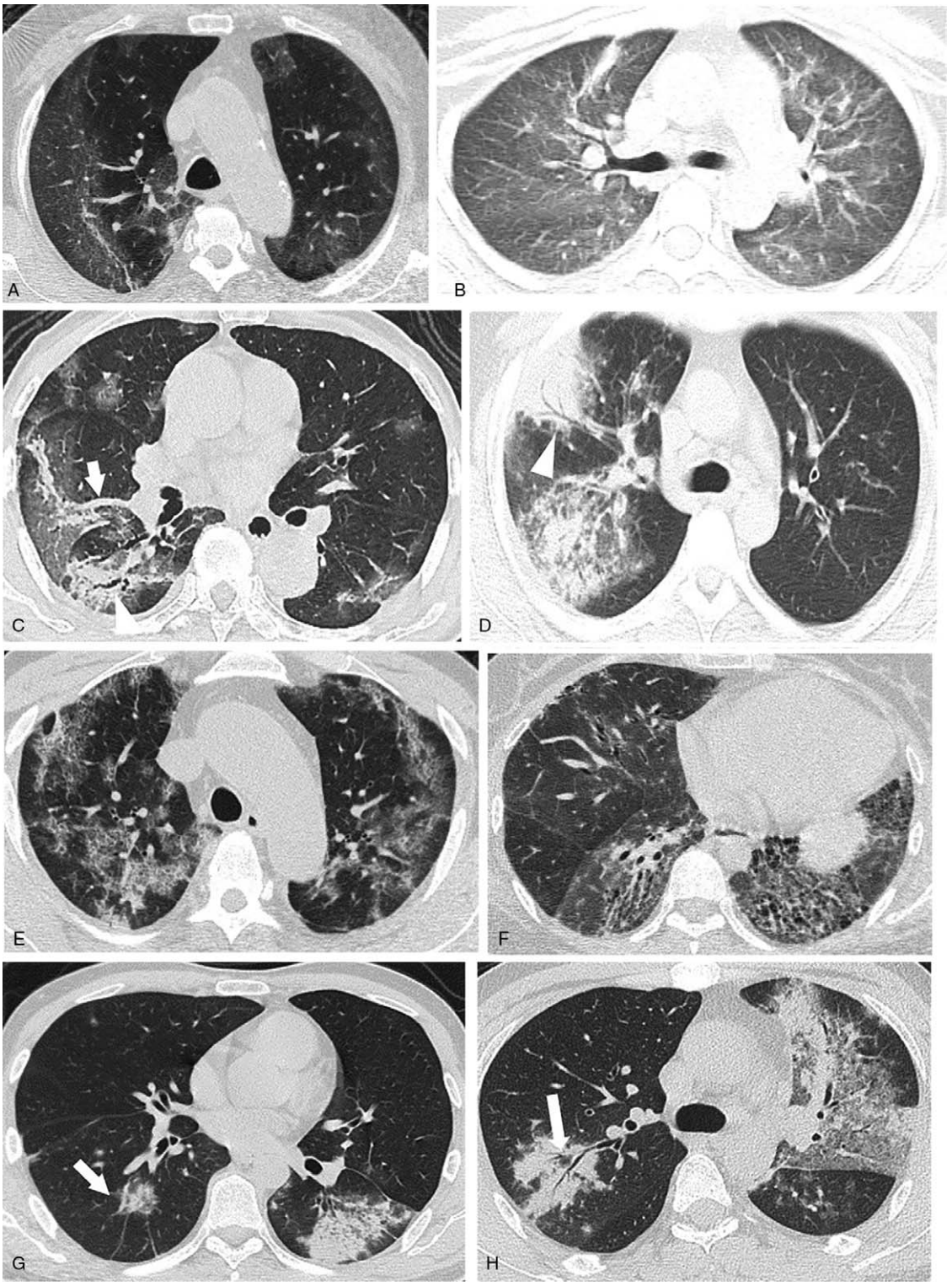

Figure 2. A, COVID-19 patient: male, 76 years old, fever for 13 days, and prominent ground glass opacities below the pleura of both lungs. B, CMV patient: female, 52 years old, cough with fever for 7 days, diffuse ground glass opacities in both lungs and central distribution. C, COVID-19 patient: male, 82 years old, fever for 3 days, mixed lesions in both lungs, partial consolidation and air bronchogram (triangular) in ground glass opacities, and thickening of peribronchovascular interstitium (arrow). D, Influenza A patient: male, 30 years old, fever and cough for 9 days, consolidation and air bronchogram in the right upper lobe. E, COVID-19 patient: male, 60 years old, fever for 9 days, multiple interlobular septal and reticular thickening in both lungs. F, EBV patient: female, 32 years old, fever for 14 days, diffuse ground glass opacities and reticular thickening in the lower lobes of both lungs. G, COVID-19 patient: male, 42 years old, fever and cough for 7 days, consolidation lesions in the left upper lobe, and nodular mixed ground glass opacities adjacent to peribronchovascular interstitial thickening (arrow) in the right lower lobe. H, Influenza A patient: male, 34 years old, fever for 7 days, large patchy mixed ground glass opacities in the left upper lobe, and larger patchy consolidation in the right upper lobe adjacent to peribronchial interstitial thickening (arrow).

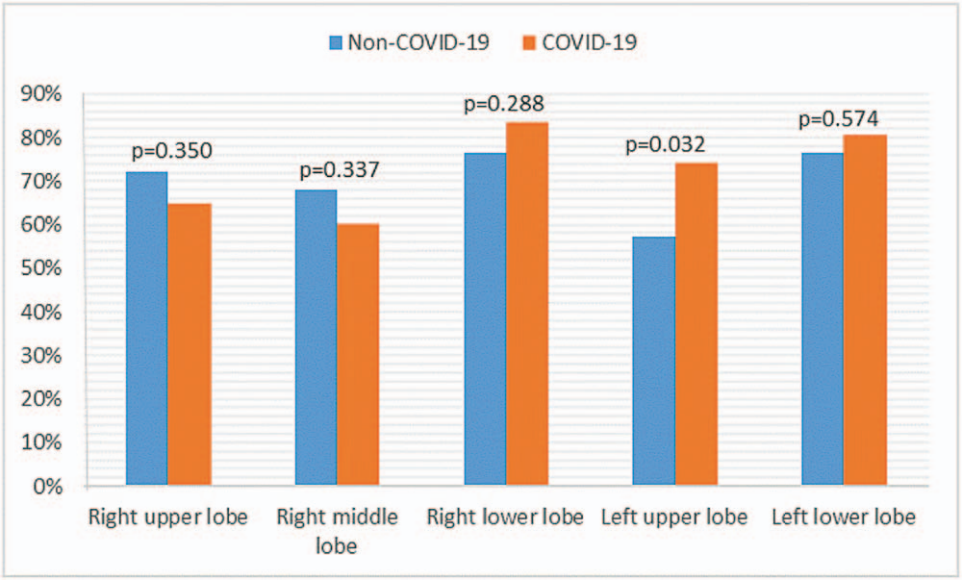

Figure 3. Comparison of the lesion involvement in different lung lobes.

glass opacities, extensive lesion distribution, mixed lesions of different sizes, and subpleural and lower lobe prominence, while peribronchial interstitial thickening was more likely to occur in non-COVID-19 viral pneumonia patients. Although viral pneumonia is caused mainly by interstitial changes, different genera of viruses have different pathogeneses, leading to different imaging changes.[12] We also found that in COVID-19 and non-COVID-19 viral pneumonia patients, the right lower lobe was more often involved, which may be related to the short and thick physiological structure of the right lower lobe bronchus that may make it easier for the virus to enter this lobe. Based on multivariable analysis, the degree of ground glass opacities, lesion distribution, lesion size, subpleural prominence, and lower lobe prominence were found to be potential independent factors to predict the probability of COVID-19 versus non-COVID-19 viral pneumonia. The specificity, sensitivity and AUC of the prediction model were 76.6%, 94.5%, and 0.91%, respectively, indicating that the model had good diagnostic efficiency and classification function. Our study will enhance radiologists understanding of COVID-19 imaging findings and further enhance the specificity of chest CT.

Our study also has some limitations. The sample size of our retrospective collection of non-COVID-19 viral pneumonia was too small, which may include some common cases and lack certain representativeness. We did not assess the consistency of the judgments made by different radiologists using the model. Although our study attempted to predict the occurrence of COVID-19 versus non-COVID-19 viral pneumonia using a more quantitative and objective approach, the recognition of image characteristics varies among radiologists with different experiences.

In conclusion, the imaging characteristics of COVID-19 and non-COVID-19 viral pneumonia are different, and the prediction model can further improve the specificity of chest CT diagnosis.

Table 3

Multivariable analysis of image feature results.

Characteristics	*P*	OR	95% CI	
			Lower	Upper
Sex	.225	1.898	0.675	5.341
GGO degree	.001*	2.078	1.346	3.210
Lesion distribution	.045*	0.527	0.281	0.987
Lesion size	.020*			
Mixed lesion	Reference			
Small lesion	.083	0.285	0.069	1.176
Large lesion	.006*	0.145	0.037	0.569
Subpleural prominence	.001*	19.461	5.916	64.015
Lower lobe prominence	.041*	3.263	1.050	10.137
Interlobular septal or reticular thickening	.374	0.527	0.128	2.166
Peribronchovascular interstitial thickening	.230	0.476	0.141	

* indicate significant *P* value.
GGO = ground glass opacities.

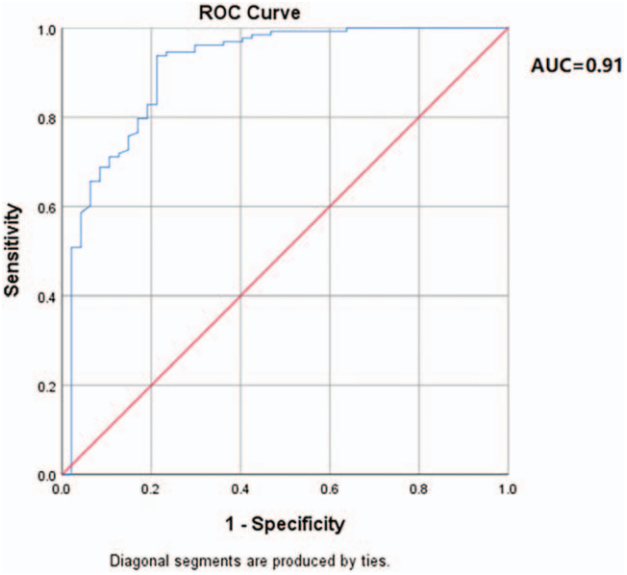

Figure 4. ROC curve of the model.

Acknowledgments:

We thank Wendong Liu, Jinshun Yao, Xingming Sang, Bin Wang for their support in data collection and statistical consultation.

Author contributions

Conceptualization: Bo Zhang, Xia Wang.
Data curation: Bo Zhang, Xia Wang, Xiaoyan Tian, Xiaoying Zhao, Bin Liu, Xingwang Wu, Yaqing Du, Guoquan Huang, Qin Zhang.
Formal analysis: Xia Wang, Xiaoyan Tian, Xiaoying Zhao.
Funding acquisition: Xingwang Wu.
Investigation: Bo Zhang, Xia Wang, Xiaoyan Tian, Xiaoying Zhao, Yaqing Du, Guoquan Huang, Qin Zhang.
Methodology: Bo Zhang, Xia Wang, Xiaoyan Tian.
Resources: Bin Liu, Xingwang Wu, Guoquan Huang.
Supervision: Bin Liu, Xingwang Wu.
Writing – original draft: Bo Zhang, Xia Wang.
Writing – review & editing: Xingwang Wu.

References

[1] World Health Organization website WHO Director-General's opening remarks at the media briefing on COVID-19. [Internet].Geneva, Switzerland [updated 2020 Mar 11; cited 2020 Mar 13] Available from: https://www.who.int/dg/speeches/detail/who-director-general-s-opening-remarks-at-the-media-briefing-on-covid-19—11-march-2020
[2] Wrapp D, Wang N, Corbett KS, et al. Cryo-EM structure of the 2019-nCoV spike in the prefusion conformation. Science 2020;367:1260–3.
[3] Fung WK, Philip LH. SARS case-fatality rates. CMAJ 2003;169:277–8.
[4] Zhao W, Zhong Z, Xie X, et al. Relation Between Chest CT Findings and Clinical Conditions of Coronavirus Disease (COVID-19) Pneumonia: A Multicenter Study. AJR Am J Roentgenol 2020;214:1072–7.
[5] Huang C, Wang Y, Li X, et al. Clinical features of patients infected with 2019 novel coronavirus in Wuhan, China. Lancet 2020;395:497–506.
[6] Xu Z, Shi L, Wang Y, et al. Pathological findings of COVID-19 associated with acute respiratory distress syndrome. Lancet Respirat Med 2020;8:420–2.
[7] Mao L, Jin H, Wang M, et al. Neurologic Manifestations of Hospitalized Patients With Coronavirus Disease 2019 in Wuhan, China. JAMA Neurol 2020;77:683–90.
[8] Fang Y, Zhang H, Xie J, et al. Sensitivity of Chest CT for COVID-19: Comparison to RT-PCR. Radiology 2020;296:E115–7.
[9] Yang Y, Yang M, Shen C, et al. Laboratory diagnosis and monitoring the viral shedding of nCoV infections. medRxiv 2020.
[10] Ai T, Yang Z, Hou H, et al. Correlation of Chest CT and RT-PCR Testing for Coronavirus Disease 2019 (COVID-19) in China: A Report of 1014 Cases. Radiology 2020;296:E32–40.
[11] Pan F, Ye T, Sun P, et al. Time Course of Lung Changes at Chest CT during Recovery from Coronavirus Disease 2019 (COVID-19). Radiology 2020;295:715–21.
[12] Koo HJ, Lim S, Choe J, et al. Radiographic and CT features of viral pneumonia. Radiographics 2018;38:719–39.
[13] Bernheim A, Mei X, Huang M, et al. Chest CT Findings in Coronavirus Disease-19 (COVID-19): Relationship to Duration of Infection. Radiology 2020;295:200463.
[14] Zhao X, Liu B, Yu Y, et al. The characteristics and clinical value of chest CT images of novel coronavirus pneumonia. Clin Radiol 2020;75:335–40.